

# Prognostic Significance of Immune and Stromal Components in Colorectal Cancer

## Practical Tools for Routine Pathologic Assessment

Mi Jang, MD, PhD; Yongki Hong, MD; Soojung Hong, MD; Eun Kyung Kim, MD, PhD

• **Context.**—In colorectal cancer (CRC), the tumor microenvironment includes cancer-associated fibroblasts and a variety of immune cells, which are increasingly recognized for their prognostic significance.

**Objective.**—To evaluate the tumor microenvironment in CRC using methodologies applicable in routine pathologic practice.

**Design.**—A comprehensive evaluation of the local immune response and tumor to stroma ratio (TSR) was performed in 930 CRC cases by thoroughly reviewing the whole hematoxylin-eosin (H&E) slides. Local immune responses were assessed using peritumoral inflammatory infiltration (Klintrup-Mäkinen and modified Klintrup-Mäkinen methods), intratumoral stromal tumor-infiltrating lymphocytes (TILs; International TILs Working Group system and deep stromal TIL system), and Crohn-like lymphoid reaction (CLR).

**Results.**—In the multivariate analysis, age (>68 years), stage III–IV, microsatellite stability, signet ring cell/undifferentiated carcinoma, extramural venous invasion, high TSR (>50%), and CLR were independent prognostic factors for disease-specific survival. Excluding microsatellite stability, these factors also served as significant prognostic indicators for progression-free survival. Among the 4 methods for measuring local immune response, evaluating the proportion of TILs within the deepest intratumoral stroma was an independent predictor of progression-free survival.

**Conclusions.**—We suggest that evaluating CLR, TSR, and stromal TILs on hematoxylin-eosin-stained slides represents a practical and straightforward approach with significant prognostic value.

(*Arch Pathol Lab Med.* 2025;149:982–990; doi: 10.5858/arpa.2024-0350-OA)

Colorectal cancer (CRC) is a prevalent malignancy worldwide and the second leading cause of cancer-related deaths after lung cancer.<sup>1</sup> Advancements in comprehending tumor biology have revealed that tumor cells, rather than being isolated, interact intricately within a complex microenvironment. This tumor microenvironment (TME) comprises 2 pivotal cellular elements, cancer-associated fibroblasts (CAFs) and diverse immune cells, which engage in intricate signaling pathways, and exhibit either protumorigenic or antitumorigenic effects through close interactions with tumor cells or among themselves.<sup>2</sup> Specifically, the local immune response within the TME, driven by the complex interplay among tumor-infiltrating lymphocytes (TILs), dendritic cells, macrophages, regulatory

T cells, myeloid-derived suppressor cells, and a multitude of immune-modulating molecules, has emerged as a crucial determinant of cancer outcomes and presents opportunities for targeted immunotherapies.<sup>3,4</sup>

Local immune responses and microsatellite instability (MSI) status are closely associated with cancer prognosis. MSI-high (MSI-H) tumors have significant instability, leading to a higher mutation burden and production of neoantigens derived from mutated proteins.<sup>5,6</sup> These neoantigens can be recognized by the immune system, triggering an enhanced immune response and resulting in a better prognosis than microsatellite-stable (MSS) tumors.<sup>7,8</sup> Immune checkpoint inhibitors have shown promising results in MSI-H CRC, providing durable responses and improving survival.<sup>4,9</sup>

The mechanism of these immune checkpoint inhibitors involves enhancing the preexisting antitumor T-cell responses, establishing them as a key therapeutic option for various cancers today. Consequently, evaluation of immune cells in the TME has recently received considerable attention and various methods have been proposed. Morphologic evaluation using hematoxylin-eosin (H&E) staining allows the determination of the overall extent, density, and distribution of immune cells.<sup>10–13</sup> In particular, the spatial distribution of immune cells within the TME, also referred to as immune cell topography, has been identified as an important predictor of prognosis and therapeutic response in CRC.<sup>14</sup> Immunohistochemistry can be effectively used to evaluate TIL subpopulations, and defining immune cell topography using specific antibodies such as CD3, CD8, CD4, FOXP3, and CD45RO and the Immunoscore

Accepted for publication February 25, 2025.

Published online March 21, 2025.

Supplemental digital content is available for this article at <https://meridian.allenpress.com/aplm> in the November 2025 table of contents.

From the Departments of Pathology (Jang, Kim), Surgery (Y. Hong), and Oncology (S. Hong), National Health Insurance Service Ilsan Hospital, Goyang-si, Republic of Korea; Department of Pathology, Yongin Severance Hospital, Yonsei University College of Medicine, Yongin-si, Republic of Korea (M. Jang).

This study was supported by the National Health Insurance Service Ilsan Hospital (grant NHIMC-2021-CR-065).

The authors have no relevant financial interest in the products or companies described in this article.

Corresponding author: Eun Kyung Kim, MD, PhD, Department of Pathology, National Health Insurance Service Ilsan Hospital, 100, Ilsan-ro, Ilsandong-gu, Goyang-si, Gyeonggi-do, 10444, Republic of Korea (email: dalsoon2@nhimc.or.kr).

scoring system is well established.<sup>15–18</sup> Multiplex immunofluorescence simultaneously detects multiple immune cell markers within tumor tissue, aiding in characterizing complex immune cell populations and understanding their spatial relationships.<sup>19,20</sup> Additionally, gene expression profiling such as RNA sequencing or microarray analysis can indirectly assess TILs through immune-related gene analysis.<sup>21,22</sup>

However, the use of these methods in clinical practice faces several barriers, such as a lack of global consensus regarding standardized protocols and cutoff values, potential interobserver variability, and the requirement for further clinical validation. A recent meta-analysis of the local inflammatory response in CRC demonstrated similar fixed-effects summaries across all evaluated immune cell types, with the exception of FoxP3 and macrophages. Moreover, the fixed effects were consistent regardless of whether H&E evaluation methods or immunohistochemistry was used to assess specific cell subtypes. The authors recommended a standardized assessment of the local inflammatory response and caution against excessive emphasis on the importance of specific immune cell subtypes.<sup>23</sup>

H&E staining may be a practical and cost-efficient approach to assess local inflammatory responses. The Klintrup-Mäkinen (KM) grade, International TILs Working Group (ITWG) system, and Crohn-like lymphoid reaction (CLR) are representative methods using H&E staining in CRC.<sup>10,13,24</sup> The KM grade assesses the density of all types of immune cells at the invasive front of the tumor, and high-KM-grade CRC patients show improved survival outcomes.<sup>25–27</sup> The ITWG system evaluates the density of mononuclear inflammatory cell infiltrates within the tumor stromal area, with a high TIL density indicating a better prognosis.<sup>13,28</sup> CLR refers to nodular lymphoid aggregates (LAs) in the peritumoral area and is associated with favorable outcomes.<sup>11,29,30</sup>

The tumor stroma, which constitutes the TME, comprises various nonneoplastic cells, including CAFs and the extracellular matrix. The tumor to stroma ratio (TSR) or tumor to stroma percentage refers to the relative proportions of tumor and intratumoral stroma.<sup>31,32</sup> This serves as a straightforward and rapid evaluation using conventional H&E-stained tissue sections, and stroma-high CRCs have demonstrated a worse prognosis.<sup>27,33–35</sup>

This study aimed to investigate the prognostic importance of the TME in CRC by evaluating the local inflammatory response and tumor stroma using methodologies applicable in routine practice. Additionally, we compared approaches for assessing the overall immune cell infiltration or TILs to determine the most effective method for clinical use and its integration into standard pathologic assessments.

## MATERIALS AND METHODS

### Patient Population

This retrospective study included patients who underwent surgery for primary CRC at the National Health Insurance Service Ilsan Hospital (Goyang-si, Republic of Korea) between 2011 and 2019. Patients who had received preoperative chemotherapy or radiation therapy and those who were found to have positive resection margins after surgery were excluded. A consecutive series of 930 patients was included in the analysis. Demographic information and follow-up data were obtained from electronic medical records. The study was conducted in accordance with the ethical principles outlined in the Declaration of Helsinki. The study protocol was approved by the Institutional Review Board

of the National Health Insurance Service Ilsan Hospital (NHIMC 2021-09-023).

### Histologic Review of Morphologic Parameters

All CRC cases were comprehensively evaluated by thoroughly reviewing H&E slides and pathology reports. This evaluation included the assessment of several parameters, including the TNM stage according to the 8th edition of the American Joint Committee on Cancer staging manual,<sup>36</sup> histologic subtypes according to the 2019 World Health Organization classification<sup>37</sup> and previous studies,<sup>38–40</sup> differentiation,<sup>41</sup> lymphovascular invasion (LVI),<sup>42</sup> extramural venous invasion (EMVI),<sup>43,44</sup> and perineural invasion. The definitions and criteria of the parameters used in this study are summarized in Table 1. The average number of slides per case was 5.4.

Tumor budding refers to the presence of individual tumor cells or small clusters of fewer than 5 cells at the leading edge of the tumor. It is a morphologic manifestation of epithelial-mesenchymal transition and is associated with poor outcomes.<sup>45,46</sup> Tumor budding was assessed based on the criteria recommended by the International Tumor Budding Consensus Conference (Table 1).<sup>47</sup> Poorly differentiated clusters (PDCs) are clusters of 5 or more tumor cells without gland formation. They are one of the manifestations of epithelial-mesenchymal transition and have been recognized as a potential prognostic indicator in CRC.<sup>45,46,48</sup> The Ueno grading system was used (Table 1).<sup>49</sup>

To assess the TSR, an area where both the tumor and stromal tissue were present was selected using a  $\times 10$  objective. Stromal ratio groups were categorized as stroma-high ( $>50\%$  stromal area) and stroma-low groups ( $\leq 50\%$  stromal area; Table 1; Figure 1, A and B).<sup>32,34</sup>

### Assessment of Peritumoral Immune Response and Intratumoral TILs Using Different Methods

We analyzed the local immune response through peritumoral inflammatory infiltration and intratumoral TIL levels. CLR and KM scores were used to represent the peritumoral inflammatory infiltration, and stromal TILs were considered to indicate intratumoral TILs (Figures 1, C through F, and 2, A through D).

CLR is defined as nodular LAs surrounding a tumor. Using previously suggested objective criteria, the presence of CLR was considered if the maximum size of at least 1 LA was 1 mm or more in diameter and the number of LAs per section was 3 or more (Table 1; Figure 1, C and D).<sup>23,30</sup>

For KM grading, we applied the conventional method<sup>11</sup> and a modified method using whole H&E slides (Table 1; Figures 1, B, and 2, A through C). The modified KM grade counts only lymphocytes and plasma cells, and excludes other types of inflammatory cells.<sup>50,51</sup>

For intratumoral stromal TILs, we used the ITWG system<sup>13,24,28,52</sup> and a modified approach by examining whole H&E-stained slides (Table 1; Figures 1, E and F, and 2, D). In contrast to the ITWG method, which evaluates the density within the entire intratumoral stromal component, the modified TIL (deep) approach exclusively assesses TIL density within the deepest invasive area at an objective magnification of  $\times 4$  (Figure 1, B).

### MSI Analysis

MSI testing was performed as a routine procedure in all resected CRC cases, excluding those with inadequate tissue amounts or poor tissue conditions; 866 cases were examined. Genomic DNA was extracted from formalin-fixed, paraffin-embedded tumor tissues and matched normal tissue sections. Five microsatellite loci (BAT25, BAT-26, D2S123, D5S346, and D17S250) recommended by the National Cancer Institute were amplified by fluorescent multiplex polymerase chain reaction and analyzed by capillary electrophoresis. MSI-H was defined as MSI at 2 or more loci, MSI low as instability at a single locus, and MSS as no instability at any of the 5 markers.<sup>53</sup>

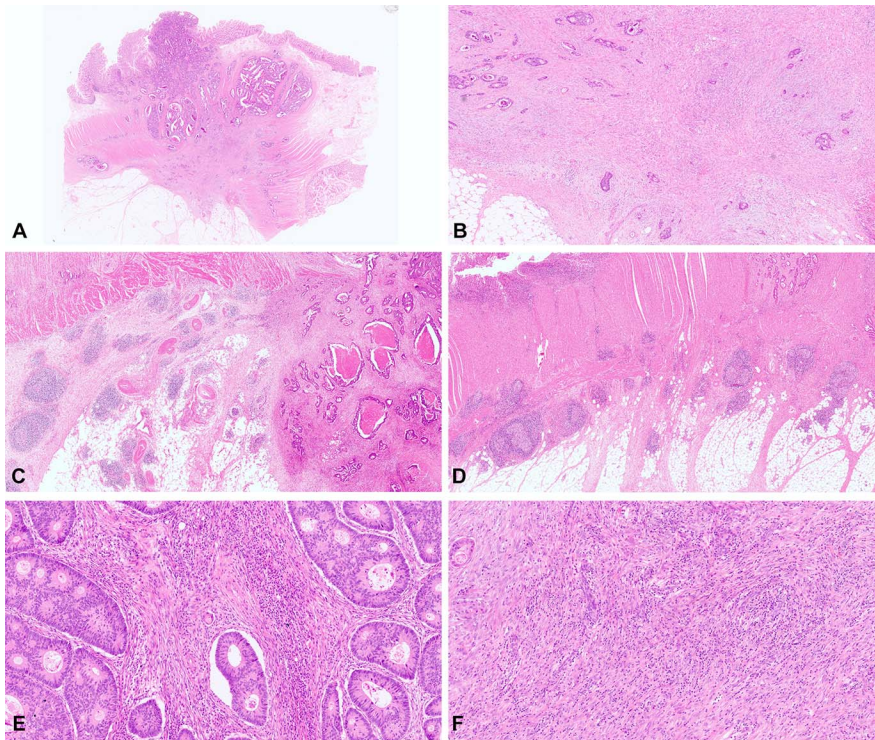
**Table 1. Histomorphologic Parameters and Their Definitions**

Morphologic Parameter	Definition
Histologic subtype	
Micropapillary ADC	Small clusters of tumor cells within stromal spaces resembling vascular channels; cutoff $\geq 5\%$
Medullary carcinoma	Sheets of tumor cells with vesicular nuclei, prominent nucleoli, and abundant eosinophilic cytoplasm. Marked infiltration by lymphocytes and neutrophilic granulocytes
Mucinous ADC	$>50\%$ of the tumor comprises pools of extracellular mucin containing evident malignant cells, including signet ring cells
Serrated ADC	1. Epithelial tufts comprise only epithelium or epithelium and basement membrane material, excluding papillary projections with a fibrovascular core and serrated-like structures resulting from tumor cell necrosis. Clear or eosinophilic cytoplasm and abundant cytoplasm, vesicular and discernible nuclei, mucin production, cell balls, papillary rods, and lack of necrosis 2. There are no established quantitative criteria for serrated ADC, and we applied a threshold of $\geq 30\%$ in the present study
Signet ring cell carcinoma	$>50\%$ of the tumor cells exhibit prominent intracytoplasmic mucin, typically leading to displacement and molding of the nucleus
Undifferentiated carcinoma	There is no morphologic, immunohistochemical, or molecular evidence of differentiation beyond that of an epithelial tumor. Lack of pushing borders, syncytial growth pattern, and prominent inflammatory cell infiltrates
Differentiation	Based on the extent of gland formation, excluding considerations of tumor budding and PDCs: well ( $>95\%$ with gland formation), moderate ( $50\%–95\%$ ), poor ( $0\%–49\%$ )
LVI	
Present	LVI refers to lymphatic invasion and intramural venous invasion, excluding extramural venous invasion
Substantial LVI	Substantial LVI denotes widespread, multifocal, or massive LVI around the tumor that is easily identifiable at low magnification
EMVI	Tumor cell invasion into veins beyond the muscularis propria. Identifying features for EMVI recognition encompass the orphan artery sign (a tumor nodule adjacent to an artery within a presumed vein) and the protruding tongue sign (tumor extension beyond its border into a vein in the surrounding fat)
Perineural invasion	Tumor cells surrounding a minimum of one-third of the nerve circumference; may exist within any of the 3 layers of the nerves (epineurium, perineurium, and endoneurium)
Tumor budding	Tumor budding refers to individual tumor cells or small clusters of fewer than 5 cells at the leading edge of the tumor
PDCs	PDCs are clusters of 5 or more tumor cells without the formation of glands and located in the tumor center and invasive front. Quantifying the number of tumor buds and PDCs within a hotspot area ( $0.950\text{ mm}^2 = \times 20$ field in microscopes with a 22-mm eyepiece FN diameter) and applying normalization factor: low ( $0–6$ ), intermediate ( $7–12$ ), and high ( $\geq 13$ ) Not counted: tumor cells suspended in pools of mucin; separation of tumor cells secondary to inflammation
Tumor to stroma ratio	Relative proportions of tumor and intratumoral stroma. The most abundant stroma is selected using the $\times 4$ objective lens. Following this, an area where both tumor and stromal tissue are present within this vision site is selected using a $\times 10$ objective. Tumor cells must be present at all borders of the selected image field. Inflammatory cells, small vessels, and hyalinization should be included; stroma high ( $>50\%$ stromal area), stroma low ( $\leq 50\%$ stromal area) Not counted: mucin, necrosis, smooth muscle tissue, glandular lumen, large vessels with a muscular wall, and tumor budding cells
CLR	Nodular LAs surrounding the tumors. A maximum diameter of LA and number of LAs per section are counted, and the presence of CLR is confirmed when there is at least 1 LA measuring 1 mm or more in diameter and the number of LAs per section is 3 or more Not counted: mucosa-associated lymphoid tissue and lymph nodes
KM grade	Overall inflammatory cell reaction (lymphocytes, plasma cells, neutrophils, eosinophils, and macrophages) on areas of deepest invasive margin Low grade (score $0–1$ ): score 0, no increase in inflammatory cells; score 1, mild and patchy increase without destruction of invading cancer cell islets High grade (score $2–3$ ): score 2, bandlike infiltrates with some destruction of cancer cell islets; score 3, prominent inflammatory reaction forming a cuplike zone with frequent and consistent destruction of cancer cell islets Not counted: area of acute inflammation or necrosis
Modified KM grade	Only mononuclear cell reaction including lymphocytes and plasma cells on areas of deepest invasive margin. Remaining methodology is unchanged Not counted: other types of inflammatory cells (eg, neutrophils and macrophages)
Stromal TIL (ITWG)	Density of mononuclear cells (lymphocytes and plasma cells) within the stromal compartment of the tumor mass on a single slide with the deepest invasion. Scored as a percentage of stromal area (rounded to the nearest 5%) based on the average across the whole slide, not focusing on hotspots. Only TILs within the borders of invasive tumors are included. The percentage is categorized into 3 groups as low ( $0\%–10\%$ ), intermediate ( $15\%–50\%$ ), and high ( $55\%–100\%$ ) Not counted: dysplastic and in situ areas, inflammation outside the tumor borders, other inflammatory cells (neutrophils and macrophages), TILs within nests of epithelial cells, zones of necrosis, fibrosis, and abscess
Stromal TIL (deep)	Density of TILs exclusively within the deepest invasive area, not considering the entire stromal component. This area corresponds to an objective magnification of $\times 4$ , using an eyepiece FN diameter of 22 mm, resulting in a field diameter of 5.5 mm and a field area of $23.76\text{ mm}^2$ ; low ( $0\%–10\%$ ), intermediate ( $15\%–50\%$ ), and high ( $55\%–100\%$ ). Remaining methodology is identical to the ITWG method

Abbreviations: ADC, adenocarcinoma; CLR, Crohn-like lymphoid reaction; EMVI, extramural venous invasion; FN, field number; ITWG, International TILs Working Group; KM, Klintrop-Mäkinen; LA, lymphoid aggregate; LVI, lymphovascular invasion; PDC, poorly differentiated cluster; TILs, tumor-infiltrating lymphocytes.



**Figure 1.** A case of T3 colon cancer (A and B) with tumor to stroma ratio 50% or greater (A). At the deepest invasive margin, both the Klintrup-Mäkinen method and the modified stromal tumor-infiltrating lymphocytes (TILs; deep) method indicate a low grade (B). Cases exhibiting Crohn-like lymphoid reaction have more than 3 nodular lymphoid aggregates surrounding the tumor, including some with a diameter greater than 1 mm (C and D). The submucosa (E) and subserosa (F) of the previously mentioned T3 colon cancer case show intermediate stromal TILs (15%–50%) according to the International TILs Working Group method (original magnifications  $\times 6$  [A],  $\times 40$  [B],  $\times 15$  [C and D], and  $\times 120$  [E and F]).



### Statistical Analysis

Descriptive statistics were used to summarize the demographic and clinical characteristics of patients. Associations between variable pathologic parameters and clinical outcomes were analyzed using

the  $\chi^2$  test or Fisher exact test. Disease-specific survival (DSS) and progression-free survival (PFS) were calculated using Kaplan-Meier curves and log-rank tests. A multivariate Cox proportional hazards model was applied using forward stepwise methods with predictive variables that were significant in the univariate analysis to identify

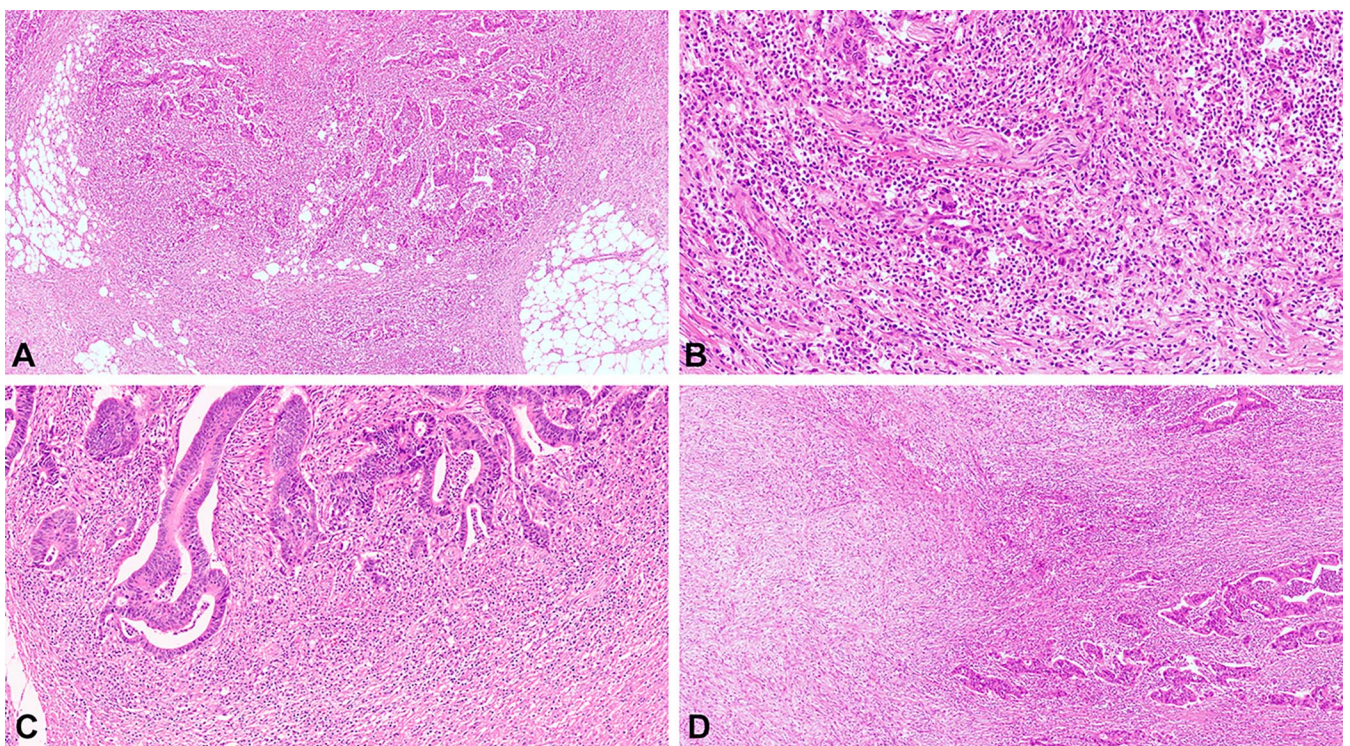


**Figure 2.** Cases of T3 colon cancer (A through D) with various inflammatory cells are heavily infiltrated, resulting in a high Klintrup-Mäkinen (KM) grade (A) and a high modified KM grade because of the abundance of lymphocytes and plasma cells (B). Despite a high KM grade, most cells are neutrophils and histiocytes, leading to a low modified KM grade (C). Spatial heterogeneity of stromal TILs (International TILs Working Group) is shown, with low on the left and intermediate on the right (D) (original magnifications  $\times 50$  [A],  $\times 200$  [B],  $\times 120$  [C], and  $\times 60$  [D]).



**Table 2. Agreement Between Assessing Methods of Peritumoral and Intratumoral Immune Response**

	KM Grade, No. (%)			$\kappa$	<i>P</i> Value
	Low	High			
Modified KM grade, No. (%)					
Low	332 (100)	49 (8.2)		.889	<.001
High	0 (0)	549 (91.8)			
	TIL (ITWG), No. (%)			$\kappa$	<i>P</i> Value
	Low	Intermediate	High		
TIL (deep), No. (%)					
Low	268 (98.9)	163 (33.6)	2 (1.1)	.633	<.001
Intermediate	3 (1.1)	308 (63.5)	36 (20.7)		
High	0 (0)	14 (2.9)	136 (78.2)		
	TIL (ITWG), No. (%)			$\kappa$	<i>P</i> Value
	Low/intermediate	High			
TIL (deep), No. (%)					
Low/intermediate	742 (98.1)	38 (21.8)		.806	<.001
High	14 (1.9)	136 (78.2)			

Abbreviations: ITWG, International TILs Working Group; KM, Klintrup-Mäkinen; TIL, tumor-infiltrating lymphocyte.

the most informative variables and calculate hazard ratios (HRs) and 95% CIs. Statistical significance was set at a 2-sided *P* value less than .05. The Cohen  $\kappa$  was used to calculate the correlation between the assessment methods for the immune response. The  $\kappa$  scores were defined as follows; less than 0.2, poor; 0.21 to 0.40, fair; 0.40 to 0.60, moderate; 0.61 to 0.80, good; and greater than 0.80, very good.<sup>54</sup> All statistical analyses were conducted using IBM SPSS version 23.0 (IBM Corp, Armonk, New York).

## RESULTS

### Clinicopathologic Characteristics

The clinicopathologic features of 930 patients with CRC are shown in Supplemental Table 1 (see supplemental digital content containing 3 tables and 2 figures at <https://meridian.allenpress.com/aplm> in the November 2025 table of contents). The mean age of the patients was 68 years, and 543 (58.4%) were men. The tumors were located in the left colon (420; 45.1%), right colon (328; 35.3%), and rectum (182; 19.6%). Stage III was the most common (534; 57.4%), followed by stages IV (201; 21.6%), II (139; 14.9%), and I (56; 6.1%). Eighty patients (9.2%) were MSI-H and 51 patients (5.9%) were MSI low. Adenocarcinoma, not otherwise specified, was the most common histologic subtype (746; 80.2%), followed by micropapillary adenocarcinoma (77; 8.3%), mucinous adenocarcinoma (55; 5.9%), serrated adenocarcinoma (25; 2.7%), medullary carcinoma (18; 1.9%), signet ring cell carcinoma (8; 0.9%), and undifferentiated carcinoma (1; 0.1%). Well-differentiated adenocarcinoma (567; 61%) was the most commonly observed, followed by moderate (263; 28.2%) and poor (100; 10.8%) differentiation.

MSI-H tumors were associated with the right colon (*P* < .001), stage I to II (*P* = .001), histologic type of mucinous carcinoma, serrated adenocarcinoma, medullary carcinoma (*P* < .001), poor differentiation (*P* < .001), low tumor budding (*P* = .001), low TSR (*P* < .001), absence of EMVI (*P* = .004), absence of perineural invasion (*P* < .001), CLR (*P* < .001), high KM grade (conventional and modified; *P* = .005

and *P* = .001), and high stromal TILs (ITWG and deep; *P* = .001; Supplemental Table 2).

High-grade tumor budding and PDC were observed in 275 (29.6%) and 266 (28.6%) patients, respectively. Tumor budding was significantly correlated with PDC (*P* < .001). In high-grade tumor budding, 61.5% and 17.5% were high-grade and low-grade PDC, respectively. PDC was significantly associated with micropapillary adenocarcinoma (*P* < .001). PDCs were high grade in 97.4% of the micropapillary adenocarcinomas, which corresponded to 28.6% of the high-grade PDCs.

The number of tumors with EMVI was 210 (22.6%), and 15 patients (1.6%) showed substantial LVI without EMVI. Perineural invasion was observed in 532 tumors (57.2%).

### Peritumoral Immune Response and Intratumoral (Stromal) TILs

The KM grades of the 930 CRC cases were low in 333 cases (35.8%) and high in 597 (64.2%). Although the modified KM grade was low in 384 patients (41.3%), it was high in 546 patients (58.7%), indicating fewer high grades than the original KM grade (Supplemental Table 1; Supplemental Figure 1, A). Agreement between KM grade and modified KM methods was very good ( $\kappa$  = 0.889, *P* < .001; Table 2). The lower grades obtained by both methods were consistent. A discrepancy was observed in 49 cases (8.2%) in which a high KM grade was a low modified KM grade (Table 2; Supplemental Figure 1, B). These patients had abundant neutrophil or macrophage infiltration and their modified KM grade was low (Figure 2, C).

The TIL (ITWG) value was low in 272 patients (29.2%), intermediate in 486 (52.3%), and high in 172 (18.5%). The number of TILs (deep) was low in 434 patients (46.7%), intermediate in 345 (37.1%), and high in 151 (16.2%). The TIL (deep) method resulted in a decreased proportion of intermediate and high grades compared with the TIL (ITWG) method (Supplemental Table 1; Figure 1, B, E, and F; Supplemental Figure 1, A). The concordance of TIL (ITWG) and TIL (deep) methods was good ( $\kappa$  = 0.633,

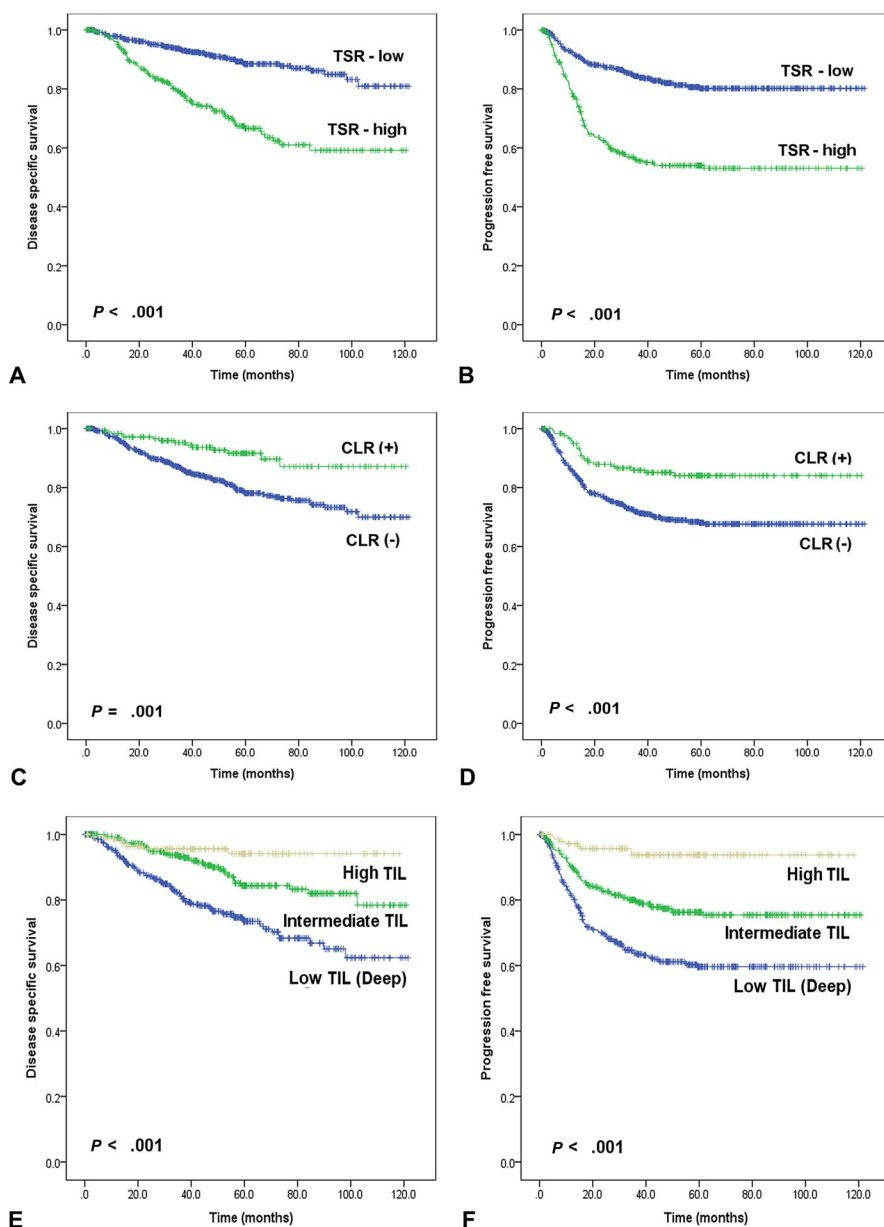


**Figure 3.** Kaplan-Meier analyses for disease-specific survival (DSS) and progression-free survival (PFS). High tumor to stroma ratio (TSR; A and B), absence of Crohn-like lymphoid reaction (CLR; C and D), and low stromal tumor-infiltrating lymphocytes (TIL [deep]; E and F) are associated with worse DSS and PFS.

$P < .001$ ; Table 2). The concordance between the 2 methods in the low and high groups was relatively high, whereas the intermediate group showed inconsistencies (Table 2). When stromal TIL values were divided into 2 groups, low/intermediate and high, the agreement became very good ( $\kappa = 0.806$ ,  $P < .001$ ; Table 2). Among the high-TIL (ITWG) group, 38 cases (21.8%) were in the low/intermediate-TIL (deep) group (Table 2; Supplemental Figure 1, B). Most of these cases were because of the heterogeneity in the distribution of stromal TILs within the tumor (Figure 2, B and D).

### Survival Impact of Various Clinicopathologic Parameters

In the univariate analysis, age ( $>68$  years), stage (I–IV), MSS, histologic subtype (micropapillary adenocarcinoma and signet ring cell/undifferentiated carcinoma), differentiation, tumor budding, PDC, TSR, LVI, perineural invasion, CLR, KM grade, modified KM grade, TILs (ITWG), and TILs (deep) were

significantly associated with DSS and PFS (Supplemental Table 3; Figure 3, A through F). The 5-year DSS rates for stages were 98% (I), 93.2% (II), 78.9% (III), and 33.1% (IV). The 5-year DSS rates for MSI-H, high TSR, and EMVI were 95.9%, 66.6%, and 55.9%, respectively. The 5-year DSS rates for CLR, high-grade KM, and high-grade TILs (ITWG) were 91.6%, 85.5%, and 95.3%, respectively (Supplemental Table 3).

In multivariate analysis with forward step procedure, age ( $>68$  years; HR, 2.25), stage III (HR, 5.63), stage IV (HR, 23.1), MSI-H (HR, 0.18), signet ring cell/undifferentiated carcinoma (HR, 19.9), poor differentiation (HR, 2.41), TSR (HR, 1.82), EMVI (HR, 2.43), and CLR (HR, 0.52) were independent prognostic factors for DSS. Age ( $>68$  years; HR, 1.64), stage III (HR, 3.13), stage IV (HR, 14.2), signet ring cell/undifferentiated carcinoma (HR, 6.87), TSR (HR, 1.46), substantial LVI (HR, 2.58), EMVI (HR, 2.08), perineural invasion (HR, 1.87), CLR (HR, 0.6), and high-grade TILs (deep, HR, 0.38) were identified as independent prognostic factors for PFS (Supplemental Table 3).

Kaplan-Meier analysis showed no significant differences in DSS and PFS between stages IIB (T4aN0M0), IIC (T4bN0M0), and III ( $P > .05$ , Supplemental Figure 2).

### Association of TSR, CLR, and TILs With Other Clinicopathologic Parameters

The TSR, CLR, and stromal TILs are morphologic indicators of the TME. The TSR and CLR were independent prognostic factors for DSS and PFS. Intratumoral stromal TIL (deep) level was independently associated with PFS when other factors were adjusted.

High TSR was associated with male sex ( $P = .04$ ), left colon ( $P = .002$ ), advanced stage (III–IV and  $P < .001$ ), MSS ( $P = .001$ ), micropapillary adenocarcinoma ( $P < .001$ ), moderate to poor differentiation ( $P < .001$ ), high-grade tumor budding ( $P < .001$ ), high-grade PDC ( $P < .001$ ), EMVI ( $P < .001$ ), perineural invasion ( $P < .001$ ), low KM grade (conventional and modified;  $P < .001$ ), and low TILs (ITWG and deep;  $P < .001$ ; Supplemental Table 1). A low TSR was significantly associated with rectal location, MSI-H, mucinous carcinoma, and medullary carcinoma (Supplemental Table 1).

CLR was correlated with stage II ( $P = .002$ ), MSI-H ( $P < .001$ ), medullary carcinoma ( $P = .003$ ), low-grade tumor budding ( $P = .01$ ), absence of LVI and EMVI ( $P < .001$ ), absence of perineural invasion ( $P = .001$ ), high KM grade (both conventional and modified;  $P = .02$  and  $P = .001$ , respectively), and high TILs (both ITWG and deep;  $P < .001$ ; Supplemental Table 1).

High TIL (deep) level was associated with younger age ( $\leq 68$  years;  $P = .03$ ), rectum ( $P = .003$ ), stage I ( $P < .001$ ), MSI-H ( $P = .003$ ), conventional adenocarcinoma and medullary carcinoma ( $P < .001$ ), being well differentiated ( $P < .001$ ), low-grade tumor budding ( $P < .001$ ), low-grade PDC ( $P < .001$ ), low TSR ( $P < .001$ ), absence of LVI or EMVI ( $P < .001$ ), absence of perineural invasion ( $P < .001$ ), CLR ( $P < .001$ ), and high KM grade (conventional and modified;  $P < .001$ ; Supplemental Table 1).

## DISCUSSION

In this study, we investigated the prognostic impact of the TME in CRC using relatively simple methods to assess the local inflammatory response and tumor stroma in routine practice.

In the multivariate analysis, age ( $> 68$  years), stage III to IV, MSI-H, signet ring cell/undifferentiated carcinoma, poor differentiation, TSR, EMVI, and CLR were independent prognostic factors for DSS. Age, stage III to IV, signet ring cell/undifferentiated carcinoma, TSR, substantial LVI, EMVI, perineural invasion, CLR, and high-grade TILs (deep) were identified as independent prognostic factors for PFS. The CLR and TSR associated with the TME were significant factors for both DSS and PFS. All 4 TIL measures were associated with DSS and PFS in univariate analysis, but only TIL (deep) level was significantly associated with PFS in multivariate analysis.

CLR correlated with stage II, MSI-H, medullary carcinoma, low-grade tumor budding, absence of EMVI, absence of perineural invasion, high KM grade, and high stromal TILs. These results are similar to previous studies, with slightly different evaluation criteria.<sup>50,55</sup> The criteria in this study included at least 1 LA measuring 1 mm or more in diameter and a minimum of 3 LAs per section. However, lowering this threshold did not achieve statistical significance. CLR has been variably defined across different studies; however, through spatial and molecular characterization, it has now been recognized as a spectrum of peritumoral LAs exhibiting varying levels of

organization and maturation. In the early stages of CLR, CD4<sup>+</sup> T cells predominantly cluster with mature antigen-presenting dendritic cells. As CLR matures, an increasing number of B cells, along with follicular dendritic cells, are recruited to form lymphoid follicles. With further organization, CLR resembles functional tertiary lymphoid structures (TLSs) containing germinal centers, which facilitate the recruitment of lymphocytes to the TME and promote a tumor-specific adaptive immune response.<sup>56</sup> There are no validated standardized criteria to date, and it appears that previous studies have occasionally used CLR and TLS interchangeably. In this study, the criterion of lymphocyte aggregates larger than 1 mm was consistently associated with germinal centers, suggesting that these can be considered TLSs.<sup>57</sup>

High intratumoral stromal TILs (deep) were associated with various favorable prognostic factors such as younger age, rectum, stage I, MSI-H, conventional adenocarcinoma and medullary carcinoma, being well differentiated, low-grade tumor budding, low-grade PDC, low TSR, absence of LVI or EMVI, absence of perineural invasion, CLR, and high KM grade.

A high TSR was associated with the left colon, advanced stage, MSS, micropapillary adenocarcinoma, moderate to poor differentiation, high-grade tumor budding, high-grade PDC, EMVI, perineural invasion, low KM grade, and low stromal TILs. A low TSR was associated with rectal location, MSI-H, mucinous carcinoma, and medullary carcinoma. High TSR is recognized as a significant negative prognostic factor and is associated with several other high-risk factors.<sup>35</sup> Therefore, evaluating the TSR is crucial, and using a 50% threshold for this evaluation is considered a practical and effective approach, even though a range of artificial intelligence–based measurement tools have been developed recently.<sup>32,58</sup>

The stronger prognostic value of TSR compared with the degree of immune cell infiltration, such as KM grade or TIL (deep), in multivariate analysis may be attributable to immune exclusion. Immune exclusion is a complex phenomenon; it refers to the inability of effector immune cells, which are recruited to the tumor periphery by chemoattraction and antigenic stimuli, to infiltrate tumor nests and eliminate cancer cells because of existing physical or biochemical barriers. It is considered one of the key mechanisms underlying primary resistance to immunotherapy.<sup>59</sup> The barriers, including the extracellular matrix, tumor vasculature, and immunosuppressive cells such as CAFs, are abundant in tumors with a high TSR, which may contribute to the development of an immunosuppressive environment and demonstrate significant clinical relevance.<sup>60</sup>

Among the methods for measuring immune cell infiltration, the agreement between the KM grade and the modified KM methods was very good. There was a discrepancy in 8.2% of the cases, in which a high KM grade was a low modified KM grade. These patients had abundant neutrophil or macrophage infiltration and their modified KM grade was low. When evaluating H&E-stained slides with the naked eye, it is not practical to count lymphocytes alone, excluding neutrophils, macrophages, and other types of inflammatory cells, when there is a mixture of different types of inflammatory cells. Therefore, we suggest that it is simpler and more reasonable to use the KM grades rather than the modified KM grades in routine diagnostics.

The concordance between the TIL (ITWG) and TIL (deep) methods was good. When the stromal TIL values were divided into 2 groups, low/intermediate and high, the agreement was very good. Heterogeneity in the distribution of stromal TILs



within the tumor was observed, with deeper intratumoral stroma generally tending to have a lower number of TILs, resulting in 21.8% being in the high group by TIL (ITWG), but in the low/intermediate group by TIL (deep). However, in practice, we believe that the TIL (deep) method, which evaluates only the stromal area of the deepest part of the tumor, is simpler and less prone to error than the ITWG method, which measures the average percentage of TILs within the entire stromal area of a tumor. Additionally, the gastrointestinal tract, which has a lumen, typically contains abundant lymphocytes in the lamina propria and often exhibits reactive inflammatory changes, such as in ulcers, in the superficial layers. Therefore, the methods for evaluating stromal TILs in gastrointestinal cancers may need to differ from those used for other solid tumors, such as breast cancer or melanoma. The aforementioned meta-analysis of the local inflammatory response in CRC revealed that, in terms of the location of immune cells, similar results were observed regardless of whether they were within the intratumoral area or at the invasive margin.<sup>23</sup> However, the implications of the spatial distribution patterns or intratumoral heterogeneity of TILs in CRC have not been extensively studied, highlighting the need for further research in this area.

MSI-H tumors were associated with right colon, stage I to II, mucinous carcinoma, serrated adenocarcinoma, medullary carcinoma, poor differentiation, low tumor budding, low TSR, and absence of EMVI, consistent with previous studies.<sup>61,62</sup> Although they also frequently exhibited CLR, high KM grade, and high stromal TILs, multivariate analysis indicated that immune infiltration factors, such as CLR or TILs, better defined the prognosis of CRC patients than MSI status.<sup>17</sup>

Tumor budding significantly correlated with PDC, and PDC was associated with micropapillary adenocarcinomas. One study suggested that the micropapillary pattern and PDC are morphologic manifestations of the same biological phenomenon and that changing evaluation of the micropapillary area to PDC may provide a more objective prognosis.<sup>63</sup> In this study, 97.4% of micropapillary adenocarcinomas were classified as high-grade PDC, and 28.6% of high-grade PDCs corresponded to micropapillary adenocarcinomas. This suggests that the micropapillary morphology may be encompassed within the concept of PDC.

Stages IIB (T4aN0M0) and IIC (T4bN0M0) were not significantly different from stage III in the Kaplan-Meier analysis. Stage II tumors at T4 without lymph node metastasis have a prognosis similar to that of stage III tumors with lymph node metastasis. Therefore, they are classified as high-risk stage II tumors and are recommended to receive adjuvant chemotherapy.<sup>64</sup>

In conclusion, our study highlights the critical role of TME-associated factors in CRC, identifying CLR and TSR as robust independent prognostic markers. Among the 4 methods for measuring local immune response, evaluating the proportion of TILs within the deepest intratumoral stroma emerged as a significant predictor of PFS. We propose that evaluating CLR, TSR, and stromal TILs in routine H&E-stained slides offers a practical and straightforward approach.

## References

1. Sung H, Ferlay J, Siegel RL, et al. Global cancer statistics 2020: GLOBOCAN estimates of incidence and mortality worldwide for 36 cancers in 185 countries. *CA Cancer J Clin*. 2021;71(3):209–249.
2. Colangelo T, Polcaro G, Muccillo L, et al. Friend or foe? The tumour micro-environment dilemma in colorectal cancer. *Biochim Biophys Acta Rev Cancer*. 2017;1867(1):1–18.
3. Shalpour S, Karin M. Pas de deux: control of anti-tumor immunity by cancer-associated inflammation. *Immunity*. 2019;51(1):15–26.

4. Le DT, Uram JN, Wang H, et al. PD-1 blockade in tumors with mismatch-repair deficiency. *N Engl J Med*. 2015;372(26):2509–2520.
5. Schwitalle Y, Kloor M, Eiermann S, et al. Immune response against frameshift-induced neopeptides in HNPCC patients and healthy HNPCC mutation carriers. *Gastroenterology*. 2008;134(4):988–997.
6. Maby P, Tougeron D, Hamieh M, et al. Correlation between density of CD8<sup>+</sup> T-cell infiltrate in microsatellite unstable colorectal cancers and frameshift mutations: a rationale for personalized immunotherapy. *Cancer Res*. 2015;75(17):3446–3455.
7. Gelsomino F, Barbolini M, Spallanzani A, Pugliese G, Cascinu S. The evolving role of microsatellite instability in colorectal cancer: a review. *Cancer Treat Rev*. 2016;51:19–26.
8. Popat S, Hubner R, Houlston RS. Systematic review of microsatellite instability and colorectal cancer prognosis. *J Clin Oncol*. 2005;23(3):609–618.
9. André T, Shiu KK, Kim TW, et al. Pembrolizumab in microsatellite-instability-high advanced colorectal cancer. *N Engl J Med*. 2020;383(23):2207–2218.
10. Klintrop K, Mäkinen JM, Kaupila S, et al. Inflammation and prognosis in colorectal cancer. *Eur J Cancer*. 2005;41(17):2645–2654.
11. Graham DM, Appelman HD. Crohn's-like lymphoid reaction and colorectal carcinoma: a potential histologic prognosticator. *Mod Pathol*. 1990;3(3):332–335.
12. Ogino S, Noshio K, Irahara N, et al. Lymphocytic reaction to colorectal cancer is associated with longer survival, independent of lymph node count, microsatellite instability, and CpG island methylator phenotype. *Clin Cancer Res*. 2009;15(20):6412–6420.
13. Fuchs TL, Sison L, Sheen A, et al. Assessment of tumor-infiltrating lymphocytes using International TILs Working Group (ITWG) system is a strong predictor of overall survival in colorectal carcinoma: a study of 1034 patients. *Am J Surg Pathol*. 2020;44(4):536–544.
14. Kather JN, Suarez-Carmona M, Charoentong P, et al. Topography of cancer-associated immune cells in human solid tumors. *Elife*. 2018;7:e36967.
15. Laghi L, Bianchi P, Miranda E, et al. CD3<sup>+</sup> cells at the invasive margin of deeply invading (pT3–T4) colorectal cancer and risk of post-surgical metastasis: a longitudinal study. *Lancet Oncol*. 2009;10(9):877–884.
16. Pagès F, Mlecnik B, Marliot F, et al. International validation of the consensus Immunoscore for the classification of colon cancer: a prognostic and accuracy study. *Lancet*. 2018;391(10135):2128–2139.
17. Mlecnik B, Bindea G, Angell HK, et al. Integrative analyses of colorectal cancer show Immunoscore is a stronger predictor of patient survival than microsatellite instability. *Immunity*. 2016;44(3):698–711.
18. Mezheyeuski A, Micke P, Martín-Bernabé A, et al. The immune landscape of colorectal cancer. *Cancers*. 2021; 13(21):5545.
19. Parra ER, Uraoka N, Jiang M, et al. Validation of multiplex immunofluorescence panels using multispectral microscopy for immune-profiling of formalin-fixed and paraffin-embedded human tumor tissues. *Sci Rep*. 2017;7(1):13380.
20. Lin J-R, Chen Y-A, Campton D, et al. High-plex immunofluorescence imaging and traditional histology of the same tissue section for discovering image-based biomarkers. *Nat Cancer*. 2023;4(7):1036–1052.
21. Gentles AJ, Newman AM, Liu CL, et al. The prognostic landscape of genes and infiltrating immune cells across human cancers. *Nat Med*. 2015;21(8):938–945.
22. Ge P, Wang W, Li L, et al. Profiles of immune cell infiltration and immune-related genes in the tumor microenvironment of colorectal cancer. *Biomed Pharmacother*. 2019;118:109228.
23. Alexander PG, McMillan DC, Park JH. The local inflammatory response in colorectal cancer—type, location or density? A systematic review and meta-analysis. *Cancer Treat Rev*. 2020;83:101949.
24. Hendry S, Salgado R, Gevaert T, et al. Assessing tumor-infiltrating lymphocytes in solid tumors: a practical review for pathologists and proposal for a standardized method from the International Immuno-Oncology Biomarkers Working Group, part II: TILs in melanoma, gastrointestinal tract carcinomas, non-small cell lung carcinoma and mesothelioma, endometrial and ovarian carcinomas, squamous cell carcinoma of the head and neck, genitourinary carcinomas, and primary brain tumors. *Adv Anat Pathol*. 2017;24(6):311–335.
25. Roxburgh CSD, Salmond JM, Horgan PG, Oien KA, McMillan DC. Comparison of the prognostic value of inflammation-based pathologic and biochemical criteria in patients undergoing potentially curative resection for colorectal cancer. *Ann Surg*. 2009;249(5).
26. Richards CH, Flegg KM, Roxburgh CS, et al. The relationships between cellular components of the peritumour inflammatory response, clinicopathological characteristics and survival in patients with primary operable colorectal cancer. *Br J Cancer*. 2012;106(12):2010–2015.
27. Park JH, McMillan DC, Powell AG, et al. Evaluation of a tumor microenvironment-based prognostic score in primary operable colorectal cancer. *Clin Cancer Res*. 2015;21(4):882–888.
28. Iseki Y, Shibutani M, Maeda K, et al. A new method for evaluating tumor-infiltrating lymphocytes (TILs) in colorectal cancer using hematoxylin and eosin (H-E)-stained tumor sections. *PLoS One*. 2018;13(4):e0192744.
29. Ueno H, Hashiguchi Y, Shimazaki H, et al. Objective criteria for Crohn's-like lymphoid reaction in colorectal cancer. *Am J Clin Pathol*. 2013;139(4):434–441.
30. Rozek LS, Schmit SL, Greenon JK, et al. Tumor-infiltrating lymphocytes, Crohn's-like lymphoid reaction, and survival from colorectal cancer. *J Natl Cancer Inst*. 2016;108(8).
31. van Pelt GW, Sandberg TP, Morreau H, et al. The tumour-stroma ratio in colon cancer: the biological role and its prognostic impact. *Histopathology*. 2018; 73(2):197–206.



32. van Pelt GW, Kjær-Frifeldt S, van Krieken JHJM, et al. Scoring the tumor-stroma ratio in colon cancer: procedure and recommendations. *Virchows Arch.* 2018;473(4):405–412.
33. Mesker WE, Junggeburst JM, Szuhai K, et al. The carcinoma-stromal ratio of colon carcinoma is an independent factor for survival compared to lymph node status and tumor stage. *Cell Oncol.* 2007;29(5):387–398.
34. Huijbers A, Tollenaar RA, v Pelt GW, et al. The proportion of tumor-stroma as a strong prognosticator for stage II and III colon cancer patients: validation in the VICTOR trial. *Ann Oncol.* 2013;24(1):179–185.
35. Gao J, Shen Z, Deng Z, Mei L. Impact of tumor-stroma ratio on the prognosis of colorectal cancer: a systematic review. *Front Oncol.* 2021;11:738080.
36. Amin MB, Edge SB, Greene FL, et al, eds. *AJCC Cancer Staging Manual*. 8th ed. New York: Springer; 2017.
37. Nagtegaal ID, Arends MJ, Odze RD, Lam AK. Tumours of the colon and rectum. In: WHO Classification of Tumours Editorial Board, eds. *Digestive System Tumours*. 5th ed. Lyon, France: International Agency for Research on Cancer (IARC); 2019:157–192. *WHO Classification of Tumours*; vol 1.
38. Haupt B, Ro JY, Schwartz MR, Shen SS. Colorectal adenocarcinoma with micropapillary pattern and its association with lymph node metastasis. *Mod Pathol.* 2007;20(7):729–733.
39. Scott N, West NP, Cairns A, Rotimi O. Is medullary carcinoma of the colon underdiagnosed? An audit of poorly differentiated colorectal carcinomas in a large national health service teaching hospital. *Histopathology.* 2021;78(7):963–969.
40. Tuppurainen K, Mäkinen JM, Junttila O, et al. Morphology and microsatellite instability in sporadic serrated and non-serrated colorectal cancer. *J Pathol.* 2005;207(3):285–294.
41. Hamilton SR, Bosman FT, Boffetta P, et al. Tumours of the colon and rectum. In: *WHO Classification of Tumours of the Digestive System*. 4th ed. Lyon, France: International Agency for Research on Cancer (IARC); 2010:134–146. *WHO Classification of Tumours*; vol 3.
42. Bosse T, Peters EE, Creutzberg CL, et al. Substantial lymph-vascular space invasion (LVSI) is a significant risk factor for recurrence in endometrial cancer—a pooled analysis of PORTEC 1 and 2 trials. *Eur J Cancer.* 2015;51(13):1742–1750.
43. Messenger DE, Driman DK, Kirsch R. Developments in the assessment of venous invasion in colorectal cancer: implications for future practice and patient outcome. *Hum Pathol.* 2012;43(7):965–973.
44. Dawson H, Kirsch R, Driman DK, Messenger DE, Assarzadegan N, Riddell RH. Optimizing the detection of venous invasion in colorectal cancer: the Ontario, Canada, experience and beyond. *Front Oncol.* 2015;4:354.
45. Pavlič A, Boštjančič E, Kavalari R, et al. Tumour budding and poorly differentiated clusters in colon cancer—different manifestations of partial epithelial-mesenchymal transition. *J Pathol.* 2022;258(3):278–288.
46. Shivji S, Cyr DP, Pun C, et al. A novel combined tumor budding-poorly differentiated clusters grading system predicts recurrence and survival in stage I–III colorectal cancer. *Am J Surg Pathol.* 2022;46(10):1340–1351.
47. Lugli A, Kirsch R, Ajioka Y, et al. Recommendations for reporting tumor budding in colorectal cancer based on the International Tumor Budding Consensus Conference (ITBCC) 2016. *Mod Pathol.* 2017;30(9):1299–1311.
48. Shivji S, Conner JR, Barresi V, Kirsch R. Poorly differentiated clusters in colorectal cancer: a current review and implications for future practice. *Histopathology.* 2020;77(3):351–368.
49. Ueno H, Hase K, Hashiguchi Y, et al. Site-specific tumor grading system in colorectal cancer: multicenter pathologic review of the value of quantifying poorly differentiated clusters. *Am J Surg Pathol.* 2014;38(2):197–204.
50. Hynes SO, Coleman HG, Kelly PJ, et al. Back to the future: routine morphological assessment of the tumour microenvironment is prognostic in stage II/III colon cancer in a large population-based study. *Histopathology.* 2017;71(1):12–26.
51. Cha YJ, Park EJ, Baik SH, Lee KY, Kang J. Clinical significance of tumor-infiltrating lymphocytes and neutrophil-to-lymphocyte ratio in patients with stage III colon cancer who underwent surgery followed by FOLFOX chemotherapy. *Sci Rep.* 2019;9(1):11617.
52. Lang-Schwarz C, Melcher B, Haumaier F, et al. Budding, tumor-infiltrating lymphocytes, gland formation: scoring leads to new prognostic groups in World Health Organization low-grade colorectal cancer with impact on survival. *Hum Pathol.* 2019;89:81–89.
53. Suraweera N, Duval A, Reperant M, et al. Evaluation of tumor microsatellite instability using five quasimonomorphic mononucleotide repeats and pentaplex PCR. *Gastroenterology.* 2002;123(6):1804–1811.
54. Landis JR, Koch GG. The measurement of observer agreement for categorical data. *Biometrics.* 1977;33(1):159–174.
55. Kim Y, Bae JM, Kim JH, Cho N-Y, Kang GH. A comparative prognostic performance of definitions of Crohn-like lymphoid reaction in colorectal carcinoma. *J Pathol Transl Med.* 2021;55(1):53–59.
56. Maoz A, Dennis M, Greenson JK. The Crohn's-like lymphoid reaction to colorectal cancer-tertiary lymphoid structures with immunologic and potentially therapeutic relevance in colorectal cancer. *Front Immunol.* 2019;10:1884.
57. He M, Ye H, Liu L, et al. Comparative analysis of tertiary lymphoid structures for predicting survival of colorectal cancer: a whole-slide images-based study. *Precis Clin Med.* 2024;18;7(4):pbac030.
58. Zhao K, Li Z, Yao S, et al. Artificial intelligence quantified tumour-stroma ratio is an independent predictor for overall survival in resectable colorectal cancer. *EBioMedicine.* 2020;61.
59. Bruni S, Mercogliano MF, Mauro FL, Cordo Russo RI, Schillaci R. Cancer immune exclusion: breaking the barricade for a successful immunotherapy. *Front. Oncol.* 2023;13:1135456.
60. Ravensbergen CJ, Polack M, Roelands J, et al. Combined assessment of the tumor-stroma ratio and tumor immune cell infiltrate for immune checkpoint inhibitor therapy response prediction in colon cancer. *Cells.* 2021;28;10(11):2935.
61. Buckowitz A, Knaebel HP, Benner A, et al. Microsatellite instability in colorectal cancer is associated with local lymphocyte infiltration and low frequency of distant metastases. *Br J Cancer.* 2005;92(9):1746–1753.
62. Greenson JK, Huang SC, Herron C, et al. Pathologic predictors of microsatellite instability in colorectal cancer. *Am J Surg Pathol.* 2009;33(1):126–133.
63. Barresi V, Branca G, Vitarelli E, Tuccari G. Micropapillary pattern and poorly differentiated clusters represent the same biological phenomenon in colorectal cancer: a proposal for a change in terminology. *Am J Clin Pathol.* 2014;142(3):375–383.
64. Baxter NN, Kennedy EB, Bergsland E, et al. Adjuvant therapy for stage II colon cancer: ASCO guideline update. *J Clin Oncol.* 2022;40(8):892–910.